JOURNAL OF VIROLOGY, Dec. 1994, p. 8131–8140
0022-538X/94/$04.00+0

Vol. 68, No. 12

Identification of the *cis*-Acting Signal for Minus-Strand RNA Synthesis of a Murine Coronavirus: Implications for the Role of Minus-Strand RNA in RNA Replication and Transcription

YI-JYUN LIN,[1] CHING-LEN LIAO,[1] AND MICHAEL M. C. LAI[1,2]*

Howard Hughes Medical Institute[2] and Department of Microbiology,[1] University of Southern California, School of Medicine, Los Angeles, California 90033-1054

Received 1 July 1994/Accepted 6 September 1994

Minus-strand RNA is the first RNA species made by plus-strand RNA viruses, such as mouse hepatitis virus (MHV), and serves as a template for subsequent RNA replication and transcription. The regulation of minus-strand RNA synthesis has been difficult to study because of the paucity of minus-strand RNA. We have optimized a ribonuclease (RNase) protection assay which enabled the detection of minus-strand RNA synthesis from nonreplicating RNAs, thus clearly separating minus-strand from plus-strand RNA synthesis. We used an MHV defective interfering (DI) RNA containing a chloramphenicol acetyltransferase gene as a reporter to determine the *cis*-acting signal for MHV minus-strand RNA synthesis. It was found that minus-strand RNAs existed in double-stranded RNA form in the cell. By using various deletion clones, we demonstrated that the *cis*-acting signal for minus-strand RNA synthesis resides in the 55 nucleotides from the 3′ end plus poly(A) tail of the MHV genome. This is much shorter than the 436 nucleotides previously reported for the 3′-end replication signal. No specific upstream MHV sequence was required for the initiation of minus-strand RNA synthesis. This finding suggests that the requirement for minus-strand RNA synthesis is much less stringent than that for genomic and subgenomic plus-strand RNA synthesis and that some of the minus-strand RNAs made may not be functional since they may lack the recognition signals for RNA replication or transcription. We further showed that the DI clones which actively transcribed a subgenomic mRNA from an internal intergenic sequence synthesized much less minus-strand RNA than those clones which did not transcribe subgenomic mRNAs, indicating that minus-strand RNA synthesis was inhibited by transcription from an internal promoter of the same DI RNA. This result also suggests that the regulation of the quantities of subgenomic mRNAs is not at the point of minus-strand RNA synthesis but rather at plus-strand RNA synthesis. Furthermore, the finding that the leader sequence was not required for minus-strand RNA synthesis suggests that the leader RNA regulates mRNA transcription during plus-strand RNA synthesis.

Minus-strand RNA synthesis represents the first step in the synthesis of various RNA species in the replication cycle of plus-strand RNA viruses. Minus-strand RNA is used as a template to synthesize genomic RNA and mRNAs during viral replication. Thus, the regulation of minus-strand RNA synthesis will impact heavily on the synthesis of plus-strand RNAs. However, the regulation of minus-strand RNA synthesis, in general, has not been well studied because the amount of viral minus-strand RNA in virus-infected cells is very small and the detection of minus-strand RNA is often complicated by the presence of an overwhelming excess of positive-strand RNA.

The study of minus-strand RNA synthesis of mouse hepatitis virus (MHV), a prototype coronavirus, is no exception. MHV contains a linear, single-stranded (ss) positive-sense genomic RNA with a size of approximately 31 kb (9, 11, 20). In virus-infected cells, seven to eight mRNAs, ranging in size from 31 to 1.8 kb, are transcribed. All of the subgenomic mRNAs are 3′ coterminal with the genomic RNA and have a nested-set structure (8), and all contain an identical leader sequence of 72 to 77 nucleotides (nt) at the 5′ end (8).

Since MHV genomic and subgenomic RNAs are of positive sense, the minus-strand RNA has to be synthesized first. These minus-strand RNAs then serve as templates for subsequent plus-strand RNA synthesis. The genomic RNA is presumably synthesized from a genomic-length minus-strand RNA template by a continuous replication process. On the other hand, the subgenomic mRNAs have to be made by a discontinuous transcription process, which fuses the leader RNA to the body sequence of mRNAs (8). Each mRNA is initiated from an intergenic (IG) site (15). The sequence requirements for both genomic RNA replication and subgenomic mRNA transcription recently have been determined (7, 13, 14). Both processes require a long stretch of *cis*-acting recognition sequences that are approximately 470 to 859 nt long, including a leader sequence at the 5′ end and 436 nt at the 3′ end. In the JHM strain of MHV, RNA replication also requires a 135-nt stretch of internal sequence (7, 14), which, however, is not required for MHV strain A59 replication (18, 27, 28). It is not clear whether the sequence requirement at the 3′ end is exclusively for the initiation of minus-strand RNA synthesis, which is a prerequisite for viral RNA replication. In addition, subgenomic transcription requires the interaction of three RNA components, i.e., *trans*- and *cis*-acting leader RNAs and IG sequences (13, 29). Some upstream sequences derived from the 5′ end of the genomic RNA are also required for subgenomic RNA transcription (13).

The major unresolved question in these transcription models is the nature of minus-strand RNA templates for subgenomic mRNA synthesis. Previously, minus-strand RNAs of the

* Corresponding author. Phone: (213) 342-1748. Fax: (213) 342-9555.

genomic- and subgenomic-sized RNAs had been detected in cells infected with several coronaviruses, including bovine coronavirus, MHV, and porcine transmissible gastroenteritis coronavirus (TGEV) (5, 21, 23, 24, 26). The minus-strand RNAs contain an antileader sequence at the 3′ end (25) and a poly(U) tract at the 5′ end (4), thus representing the authentic complementary copies of viral mRNAs. Furthermore, the relative amounts of various subgenomic minus-strand RNAs correspond to those of mRNAs. Thus, it was suggested that regulation of mRNA transcription is done at the step of minus-strand RNA synthesis and that mRNAs are synthesized by amplification of the subgenomic minus-strand RNAs or transcription from these templates (26). Several models have been proposed to explain the synthesis of these subgenomic minus-strand RNAs (24, 26). In contrast, another model of coronavirus transcription, the leader-primed transcription model, states that the RNA template for subgenomic transcription is the full-length minus-strand RNA and that the discontinuous synthesis step occurs during plus-strand rather than minus-strand RNA synthesis (8). Although these models are not mutually exclusive, the step of regulation of RNA synthesis is different between these models. It should be noted that subgenomic mRNAs do not contain the entire *cis*-acting signals for either transcription or replication (7, 13, 14). Thus, the functional significance of the minus-strand RNA copies of subgenomic mRNAs is not clear. To resolve these issues, it is important to determine the sequence requirement and regulation of minus-strand RNA synthesis. In this communication, we have developed a sensitive RNase protection assay and utilized a DI RNA reporter (chloramphenicol acetyltransferase [CAT]) system to directly examine the *cis*-acting signals for minus-strand RNA synthesis. We have demonstrated that MHV minus-strand RNA synthesis requires a surprisingly short RNA sequence at the 3′ end, which is much shorter than the 3′-end sequence requirement for RNA replication. No specific viral 5′-end sequences are required. This finding explains the generation of subgenomic minus-strand RNAs. Our findings also revealed interesting insights into the mechanism of regulation of MHV RNA replication and transcription.

MATERIALS AND METHODS

Viruses and cells. The A59 strain (17) of MHV (MHV A59) was used as a helper virus throughout this study. All of the experiments and virus stock preparation were performed on DBT cells, a murine astrocytoma cell line (3).

Construction of plasmids. (i) Prototype DI construct. The 25CAT prototype DI construct, which contains a CAT gene placed behind an IG sequence, has been described previously (13). Clones 25CAT/RIS (lacking an IG sequence [13]), 25CATΔApaI, 25CATΔHincII, 634CAT, 541CAT, 538CAT, LStuCAT, L6CAT, and LCAT (see Fig. 6A and 7A) were derived from 25CAT as described previously (13).

(ii) ADI2-CAT and its derived clones. The previously described AF3-CAT clone (14) was renamed ADI2-CAT for the sake of consistent nomenclature. ADI2CATΔSalBsu and ADI2CATΔSphApa (see Fig. 2A) were generated by deleting the *Sal*I-*Bsu*36I and *Sph*I-*Apa*I fragments, respectively, from ADI2-CAT, by blunt-ending the sequence with T4 DNA polymerase, and by self-ligation with T4 DNA ligase.

(iii) 3′-end serial deletion clones of 25CAT. To construct the 3′-end serial deletion clones of 25CAT, 7.5 μg of 25CAT plasmid DNA was first digested with *Bsu*36I and *Pst*I and then progressively digested toward both ends by using the Erase-a-Base system (Promega) as described previously (14). Briefly, the *Bsu*36I- and *Pst*I-cut plasmid DNA was digested with exonuclease III for 1 to 8 min at 15°C; an aliquot of the reaction mixture was removed at 1-min intervals, and the reaction of the removed sample was stopped immediately by mixing with S1 nuclease digestion buffer at 4°C. The DNA samples were blunt ended by treatment with S1 nuclease and Klenow enzyme, as suggested by the manufacturer (Promega). The resulting DNA was self-ligated with T4 DNA ligase (Boehringer Mannheim) and transformed into *Escherichia coli* DH5α. All clones thus obtained were sequenced across the junction points with an upstream and a downstream primer by using the Sequenase system (U. S. Biochemical).

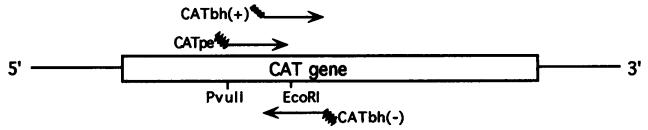

FIG. 1. Schematic representation of CAT gene probes. The orientations and positions in the CAT gene of CATpe, CATbh(+), and CATbh(−) probes are shown by arrows. Heterologous sequences derived from the vector are shown by wavy lines. The *Pvu*II and *Eco*RI sites of the CAT gene are indicated.

(iv) Probe clones. For pBS-CATpe, the *Pvu*II-*Eco*RI fragment (104 nt in length) of the CAT gene was isolated from the pCAT-Basic plasmid DNA (Promega) and ligated into the *Eco*RV-*Eco*RI-digested pBluescript-SK(−) vector (Stratagene) to generate pBS-CATpe. The transcript from the T7 promoter of this plasmid was in the plus-strand CAT gene sense. For pGem-CATbh, the CATbh DNA fragment was made by PCR with pCAT-Basic plasmid DNA and two oligonucleotide primers, LA951 (5′-ACGGATCCGGCCTTTAT TCACATT-3′) and LA952 (5′-GTGTTAACAAGGGTGAA CACTAT-3′). The underlined nucleotides are *Bam*HI and *Hin*cII recognition sequences, respectively. PCR was carried out for 30 cycles of reactions at 94, 58, and 72°C for 1 min each. The amplified fragment was digested with *Bam*HI and *Hin*cII and ligated into the *Bam*HI- and *Hin*cII-digested pGem-3Zf(−) vector (Promega) to generate pGem-CATbh. The RNAs transcribed from T7 and SP6 promoters were in the plus- and minus-strand CAT gene sense, respectively.

In vitro transcription of RNA and riboprobe. To synthesize RNAs used for transfection, 0.5 μg of *Xba*I-linearized plasmid DNA was transcribed with 40 U of T7 RNA polymerase (Promega) by the procedure recommended by the manufacturer. The nucleic acids were extracted with phenol-chloroform, precipitated with ethanol, and resuspended in *Eco*RI restriction enzyme digestion buffer. After addition of 5 U of *Eco*RI DNase and 20 U of RQ1 DNase (RNase-free DNase I; Promega), the reaction mixture was incubated at 37°C overnight. Exonuclease III (100 U; Boehringer Mannheim) was then added, and the reaction was carried out for another 30 min at 37°C. For CATpe riboprobe transcription, 0.5 μg of *Eco*RI-linearized pBS-CATpe plasmid DNA was transcribed with 40 U of T7 RNA polymerase in the presence of 70 μCi [^{32}P]UTP (3,000 Ci/mM; ICN Biochemicals), treated with 20 U of RQ1 DNase at 37°C overnight, and purified by passage through a G50 spin column (5 prime → 3 prime, Inc.). The 160-nt riboprobe thus transcribed contained a 56-nt vector sequence at the 5′ end and a 104-nt CAT gene sequence at the 3′ end (Fig. 1). For the CATbh(+) and CATbh(−) riboprobe preparations, 0.5 μg of pGem-CATbh plasmid DNA was digested with *Hin*cII and *Bam*HI and transcribed with T7 and SP6 RNA polymerase (Promega), respectively. After transcrip-

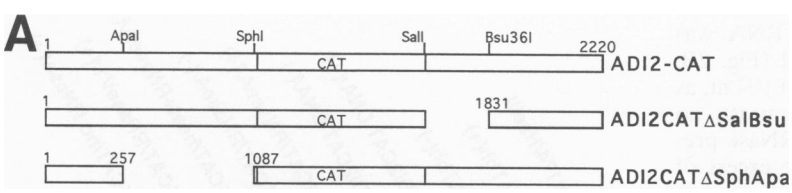

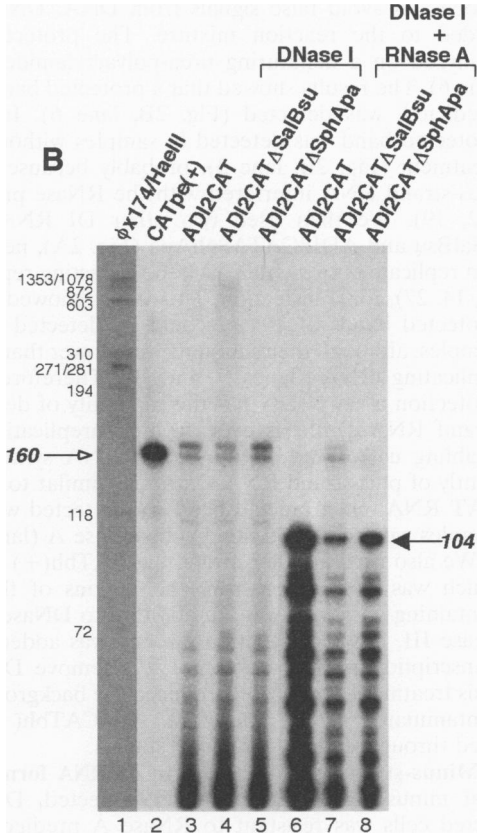

FIG. 2. RNase protection assay of minus-strand RNA synthesized by ADI2-CAT and its derived clones. (A) Schematic diagrams of structures of ADI2-CAT and its derived clones. Cloning sites on ADI2-CAT are indicated. The nucleotide numbers correspond to those of the DNA clone of DIssE (16). (B) The cytoplasmic RNAs were pretreated with DNase I (lanes 3 to 5) or DNase I plus RNase A (lanes 6 to 8) and then analyzed by RNase protection assay to detect minus-strand RNA (see the text for details). The input ^{32}P-labeled CATpe probe (lane 2) is indicated by an open arrow. The protected fragment is indicated by a closed arrow. *Hae*III-digested, ^{32}P-end-labeled φx174 RF DNA fragments were run in lane 1 as size markers. The sizes of the probe, the protected band, and the size markers are given in number of nucleotides. Computer images were generated by Adobe Photoshop, version 2.5.1 LE.

tion, the template DNA was digested with RQ1 DNase, and the riboprobes were purified by the same procedure described above. The 135-nt CATbh(+) and the 138-nt CATbh(−) probes contained 27- and 30-nt vector sequences, respectively, at the 5′ end, and both contained a 108-nt CAT gene sequence at the 3′ end (Fig. 1).

RNA isolation and RNase protection assays. To detect minus-strand RNA synthesis in vivo, approximately 10^6 DBT cells in a well of a six-well plate were infected with MHV-A59 at a multiplicity of infection of 10. The infected cells were transfected with 5 μg of in vitro-transcribed RNA at 1 h postinfection (p.i.) by using *N*-[1-(2,3-dioleoyloxy)propyl]-*N*,*N*,*N*-trimethylammoniummethylsulfate (DOTAP; Boehringer Mannheim) and then incubated at 37°C for 6 h in most of the experiments or for various lengths of time in kinetic studies. To harvest viral RNA, cells were washed two times with ice-cold NTE buffer (100 mM NaCl, 10 mM Tris-HCl [pH 8.0], 1 mM EDTA) and treated with 0.25 ml of NTE-Nonidet P-40 lysis buffer (0.5% [vol/vol] Nonidet P-40 in NTE) for 10 min. The lysate was clarified of cell debris by brief centrifugation, and the supernatant was treated with DNase I (10 μg/ml; U. S. Biochemical) and, where indicated, RNase A (0.5 μg/ml; U. S. Biochemical) for 30 min at 37°C. Sodium dodecyl sulfate (SDS) (1% [vol/vol]) was added to terminate the reaction. Proteinase K was then added to a final concentration of 100 μg/ml, and the reaction mixture was incubated for 1 h at 37°C. In one of the experiments, RNase V1 (5.6 U/ml; U. S. Biochemical) was added to the RNA sample, and the reaction was incubated overnight at 37°C. The mixture was extracted with phenol-chloroform, and the RNA was precipitated and subjected to RNase protection assay as described previously (10, 22). Briefly, 20 to 40 μg of precipitated RNA was resuspended in 30 μl of hybridization buffer (40 mM PIPES [piperazine-*N*-*N*′-bis(2-ethanesulfonic acid; pH 6.7], 400 mM NaCl, 1 mM EDTA, 80% [vol/vol] formamide) containing 2×10^5 cpm ^{32}P-labeled RNA probe. The hybridization mixture was heated at 85°C for 10 min and then incubated at 45 to 50°C for 12 to 15 h. After hybridization, 300 μl of RNase digestion solution containing 10 μg of RNase A per ml and 0.5 μg of RNase T_1 (U. S. Biochemical) per ml in 10 mM Tris-HCl (pH 7.5)–5 mM EDTA–300 mM NaCl was then added, and the reaction mixture was incubated at 30°C for 15 min. Proteinase K (100 μg/ml) and SDS (1% [vol/vol]) were added, and the reaction mixture was incubated at 37°C for 1 h. The mixture was extracted with phenol-chloroform, and the RNA was precipitated and resuspended in 10 μl of loading dye (80% formamide, 10 mM EDTA, 0.1% [wt/vol] bromophenol blue, 0.1% [wt/vol] xylene cyanol FF). The samples were then heat denatured, run on a 6% polyacrylamide gel containing 7.66 M urea, dried, and exposed to X-ray film (Kodak).

RESULTS

Detection of minus-strand RNA synthesis from replicating and nonreplicating DI RNAs. Previously, minus-strand RNAs have been detected in coronavirus-infected cells by either metabolic labeling or Northern (RNA) blot analyses (5, 21, 23, 26). In general, minus-strand RNA could be detected at 2 to 3 h after infection, when minus-strand RNA became more abundant. To determine the sequence requirement and mechanism of regulation of minus-strand RNA synthesis, we first studied the feasibility of developing a more sensitive method to detect minus-strand RNA synthesis. For this purpose, we used a CAT gene-containing DI RNA vector (ADI2-CAT), which can replicate in MHV-infected cells (14) (data not shown), as a test RNA, and a ^{32}P-labeled CATpe RNA (Fig. 1), which is complementary to minus-strand CAT RNA, as a probe. The in vitro-transcribed ADI2-CAT RNA was transfected into A59-infected DBT cells, and the cytoplasmic RNA was harvested at 7 h p.i. We then used a modified two-cycle RNase protection assay (12, 19), in which cytoplasmic RNA from virus-infected cells was pretreated with RNase, purified, and subjected to RNase protection assay. The RNA samples harvested from the ADI2-CAT-transfected, A59-infected cells were first treated with RNase A prior to hybridization with the ^{32}P-labeled

probe. To avoid false signals from DNA, DNase I was also added to the reaction mixture. The protected RNA was analyzed on a denaturing urea-polyacrylamide gel (Fig. 2B, lane 6). The results showed that a protected band of 104 nt, as predicted, was detected (Fig. 2B, lane 6). In contrast, no protected band was detected in samples without RNase pretreatment (Fig. 2B, lane 3), probably because the excess of plus-strand RNA interfered with the RNase protection assay (12, 19). We then used two other DI RNAs, ADI2CAT ΔSalBsu and ADI2CATΔSphApa (Fig. 2A), neither of which can replicate because they lack the *cis*-acting replication signal (7, 14, 27), for transfection. The results showed that the same protected bands of 104 nt could be detected in both RNA samples, although their amounts were lower than that from the replicating RNA (lanes 7 and 8). Therefore, our RNase protection assay clearly has the capability of detecting minus-strand RNA synthesis even from nonreplicating DI RNAs, enabling us to study minus-strand RNA synthesis independently of plus-strand RNA synthesis. Similar to that in ADI2-CAT RNA, no protected band was detected when the RNA samples were not pretreated with RNase A (lanes 4 and 5).

We also used another probe, the CATbh(+) RNA (Fig. 1), which was transcribed from the regions of the CAT gene containing an *Eco*RI site. In addition to DNase I and exonuclease III, *Eco*RI restriction enzyme was added to the RNA transcription mixture to completely remove DNA template. This treatment significantly reduced the background caused by contaminated DNA. Therefore, the CATbh(+) probe was used throughout the rest of the studies.

Minus-strand RNAs existed in ds RNA form. The finding that minus-strand RNA in MHV-infected, DI RNA-transfected cells was resistant to RNase A predigestion (Fig. 2) suggested that minus-strand RNA was present in double-stranded (ds) RNA form. This interpretation is also consistent with published reports (21, 23). To further characterize the nature of minus-strand RNA, we used another DI clone, 25CAT, which can synthesize a full-length RNA and transcribe a subgenomic mRNA (13), for further studies. In vitro-transcribed 25CAT RNA was transfected into A59-infected cells, and the cytoplasmic RNA was harvested. If the RNase-resistant RNA indeed represented an authentic ds RNA but not a random RNA aggregate, it should contain both minus- and plus-strand RNAs in equal amounts. Therefore, ^{32}P-labeled CATbh(+) and CATbh(−) probes were hybridized separately to the RNase A-predigested RNA samples in the RNase protection assay. The quality of the RNA probes was determined by hybridization to the DNA template, which showed a protected fragment of the same size (Fig. 3, lanes 4 to 5). The weaker signal of the protected CATbh(−) probe (Fig. 3, lane 5) was probably due to the lower specific radioactivity of the CATbh(−) probe (compare lanes 4 and 5), which contains a smaller number of U residues than the CATbh(+) probe, and also differences in the hybridization abilities between the CATbh(+) and CATbh(−) probes to the target template. Regardless, hybridization of these two probes to the RNase A-predigested RNA samples from MHV-infected, 25CAT RNA-transfected cells showed that both plus- and minus-strand RNA probes yielded bands of the same size and comparable molar amounts, considering their relative specific activities (Fig. 3, lanes 6 and 7). Furthermore, when the RNA sample was treated with RNase V1 (lane 9), which is a ds-RNA-specific RNase, or heat-denatured before RNase A digestion (lane 8), no protected RNA band was detected. As previously shown, the protected RNA band could not be detected without prior RNase digestion (lane 10). These results clearly indicated that MHV minus-strand RNAs were present in ds RNA form, confirming the previous results (21, 23).

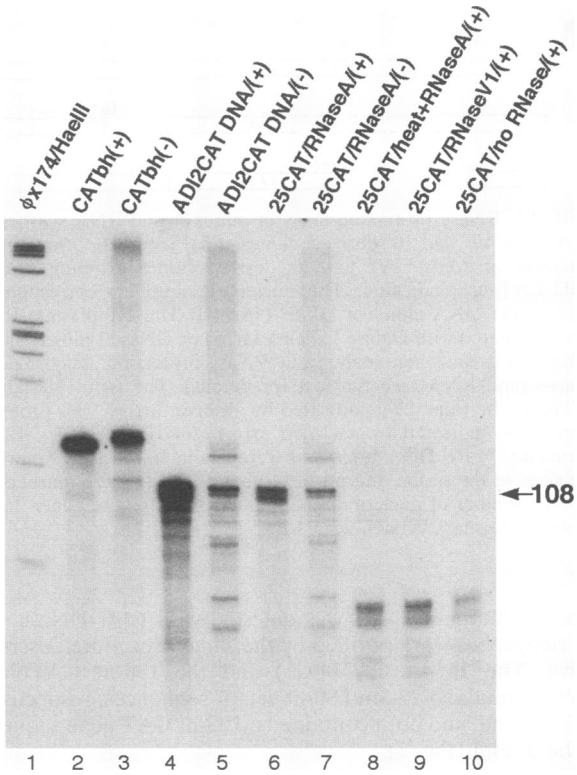

FIG. 3. RNase A-resistant RNAs. The cytoplasmic RNA from MHV-infected, 25CAT RNA-transfected cells was subjected to various pretreatments (lanes 6 to 9) or no treatment (lane 10) and then hybridized to the ^{32}P-labeled CATbh(+) (lanes 6 and 8 to 10) or CATbh(−) (lane 7) probe in the RNase protection assay. The input CATbh(+) and CATbh(−) probes are shown in lanes 2 and 3, respectively. As positive controls, ADI2-CAT DNA was used for hybridization to CATbh(+) and CATbh(−) probes in RNase protection assay (lanes 4 and 5, respectively). *Hae*III-digested, ^{32}P-end-labeled φx174 RF DNA fragments were run in lane 1 as size markers. The protected band is indicated by a solid arrow; its size is given in number of nucleotides. Computer images were generated by Adobe Photoshop, version 2.5.1 LE.

Kinetic studies showed that DI minus-strand RNA synthesis was an immediate-early event after RNA transfection. It had been shown previously that coronavirus minus-strand RNAs of genomic and subgenomic sizes were detectable from 2 to 3 h p.i. and were synthesized continuously throughout viral infection, with peaks at 5 to 6 h p.i. for MHV A59 (23) or at 4 h p.i. for TGEV (26). The RNase protection assay provided a more sensitive method for determining the kinetics of MHV minus-strand RNA synthesis. In vitro-synthesized 25CAT DI RNA was transfected into A59-infected cells, and the cytoplasmic RNA was harvested at various time points after transfection and analyzed by RNase protection assay (Fig. 4). Interestingly, the DI minus-strand RNA could be detected as early as 20 min after transfection and reached a plateau as early as 2 h p.i. (or 1 h posttransfection) (Fig. 4A, lanes 5 to 9). From 2 to 7 h p.i. (or 1 to 6 h posttransfection), the amount of minus-strand RNA did not increase (Fig. 4B). The leveling of the amount of minus-strand RNA was not due to saturation of the input CATbh(+) probe, because, in the control experiments, up to 1 ng of the in vitro-transcribed minus-strand ADI2-CAT RNA

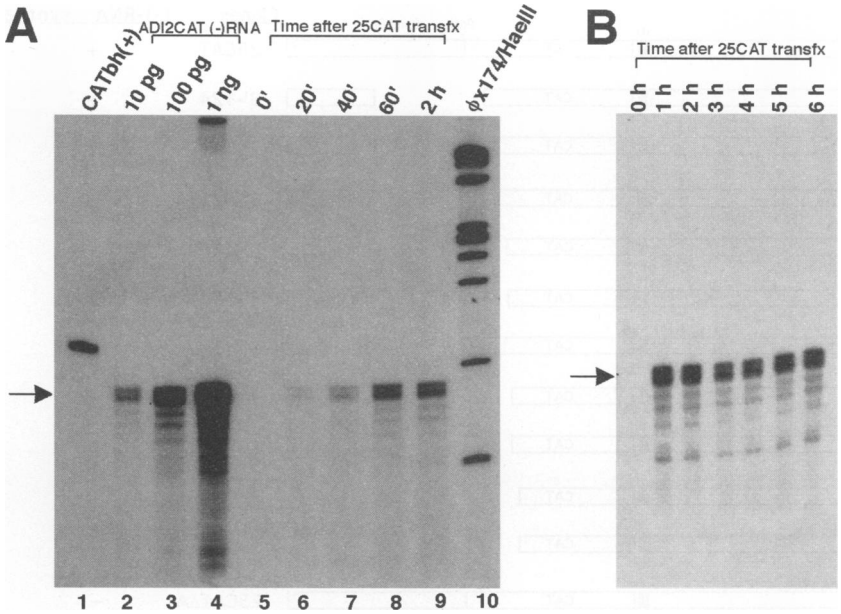

FIG. 4. Kinetic studies of minus-strand RNA synthesis of 25CAT. (A) Cytoplasmic RNA from 25CAT-transfected (transfx) cells was isolated at 0 min (lane 5), 20 min (lane 6), 40 min (lane 7), 1 h (lane 8), and 2 h (lane 9) posttransfection and analyzed by RNase protection assay. For quantitative comparison, 10 pg (lane 2), 100 pg (lane 3), and 1 ng (lane 4) of in vitro-transcribed minus-strand ADI2-CAT RNA were used in RNase protection assay. (B) Detection of minus-strand RNA at hourly intervals after 25CAT RNA transfection. The protected band is indicated by solid arrows. Computer images were generated by Adobe Photoshop, version 2.5.1 LE.

could be readily detected (Fig. 4A, lanes 2 to 4), but the harvested cytoplasmic RNA reached a plateau comparable to less than 100 pg of minus-strand ADI2-CAT RNA. Our results indicated that 25CAT minus-strand RNA synthesis occurred immediately but stopped not long after transfection. This observation was different from that seen with minus-strand RNA synthesis of A59- and TGEV-infected cells (23, 26). It should be noted that, in our experiments, cells were infected with A59 virus 1 h before transfection of DI RNA. This result suggests that viral RNA polymerase had been synthesized during the 1-h period and that the transfected DI RNAs could be used as templates to synthesize minus-strand RNA immediately after their introduction into the cells. Further minus-strand RNA synthesis was inhibited probably because transcription of the subgenomic mRNA from this RNA inhibited minus-strand RNA synthesis (see below). This result indicates that minus-strand RNA synthesis is a very rapid and early event in viral RNA synthesis.

A sequence as short as 55 nt plus poly(A) from the 3′ end of MHV genome was sufficient to initiate minus-strand RNA synthesis. As shown in Fig. 2, the two RNAs, ADI2CAT ΔSalBsu and ADI2CATΔSphApa, which could not replicate because of the lack of a complete signal for viral RNA replication (7, 14, 27), still synthesized minus-strand RNA, although the signals were weaker than that of the replicating ADI2-CAT RNA. This finding suggests that the complete RNA replication signal is not required for minus-strand RNA synthesis. To determine the *cis*-acting signal for minus-strand RNA synthesis, we first constructed a series of 3′-end deletion clones of 25CAT to study the minimum sequence requirement at the 3′ end. The 25CAT plasmid DNA was cut at the *Pst*I site, which was inserted immediately downstream of the CAT gene during construction, and the *Bsu*36I site, which was located 378 nt from the 3′ terminus. The *Pst*I-*Bsu*36I-digested 25CAT DNA was then treated with exonuclease III to serially delete sequences toward both orientations. All but one (25CATΔ3′-0ΔA) of the clones also contained a poly(A) tail. The resulting clones (Fig. 5A) were examined for their abilities to make minus-strand RNA. Among these clones, 25CATΔ3′-124, 25CATΔ3′-111, 25CATΔ3′-92, 25CATΔ3′-76, and 25CATΔ3′-55 showed a protected band with the expected size, whereas 25CATΔ3′-45, 25CATΔ3′-33, 25CATΔ3′-26, 25CATΔ3′-0, and 25CATΔ3′-0ΔA did not (Fig. 5B and data not shown). These results indicated that the minimum *cis*-acting signal for minus-strand RNA synthesis resides within 55 nt from the 3′ end. Most of these RNA samples also yielded two RNA bands corresponding to the size of the probe. They were likely the results of RNA aggregation and were not consistently observed.

The 3′ ends of MHV genomic, subgenomic, and DI RNAs contain a stretch of poly(A) sequence. Correspondingly, the 5′ end of minus-strand RNAs of bovine coronavirus contains a poly(U) sequence (4). To determine whether the poly(A) tail plays a role in minus-strand RNA synthesis, a mutant clone, 25CATΔA, in which the poly(A) tract of 25CAT is deleted, was examined for the ability to synthesize minus-strand RNA (Fig. 5C). In contrast to 25CAT, the minus-strand RNA of 25CATΔA was not detected (Fig. 5C, compare lanes 4 and 5), suggesting that the poly(A) tail of MHV RNA is important for the synthesis of minus-strand RNA. These results, taken together, demonstrated that the 55 nt from the 3′ end plus poly(A) tail of the MHV genome constitutes the minimum *cis*-acting signal at the 3′ end for minus-strand RNA synthesis.

The 5′-end MHV RNA sequences were not required for minus-strand RNA synthesis. The genomic RNA and all subgenomic mRNAs contain a leader sequence at the 5′ end; furthermore, the leader sequence and some other sequences derived from the 5′ end of the genomic RNA, in addition to the leader RNA, are required for MHV RNA replication and transcription (7, 13, 14, 27, 28). Therefore, it is important to determine the sequence requirement at the 5′ end of DI RNA for minus-strand RNA synthesis. This information will reveal

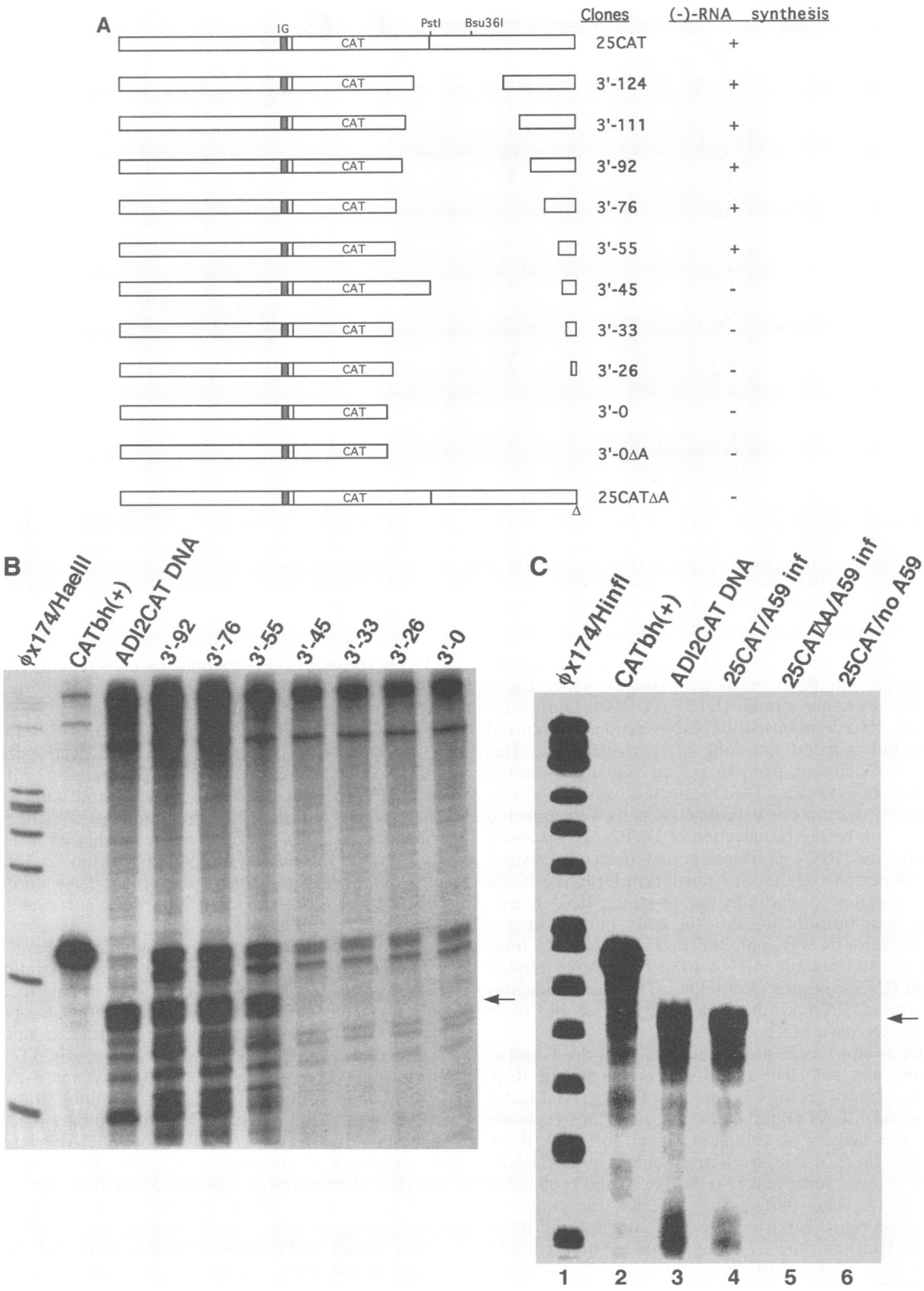

FIG. 5. Minus-strand RNA synthesis of the 3′-end deletion clones. (A) Schematic diagram of the structure of the 3′-end deletion clones. The number at the end of each clone indicates the number of virus-specific nucleotides left at the 3′ end. The poly(A) tails of 25CATΔ3′-0ΔA and 25CATΔA were deleted. The *Pst*I and *Bsu*36I sites and the IG sequence on 25CAT are indicated. The abilities of the clones to synthesize minus-strand RNA are summarized to the right of each clone. (B) Analysis by RNase protection assay of minus-strand RNA synthesis of the 3′-end deletion clones. (C) RNase protection analysis of a poly(A) deletion mutant. The RNA used for transfection and A59 infection (lanes 4 and 5) or mock infection (lane 6) are indicated above each lane. *Hin*fI-digested, ^{32}P-end-labeled φx174 RF DNA fragments were run in lane 1 as size markers. Lanes: 2, probe only; 3, hybridization to DNA. The protected band is indicated by a solid arrow. Computer images were generated by Adobe Photoshop, version 2.5.1 LE.

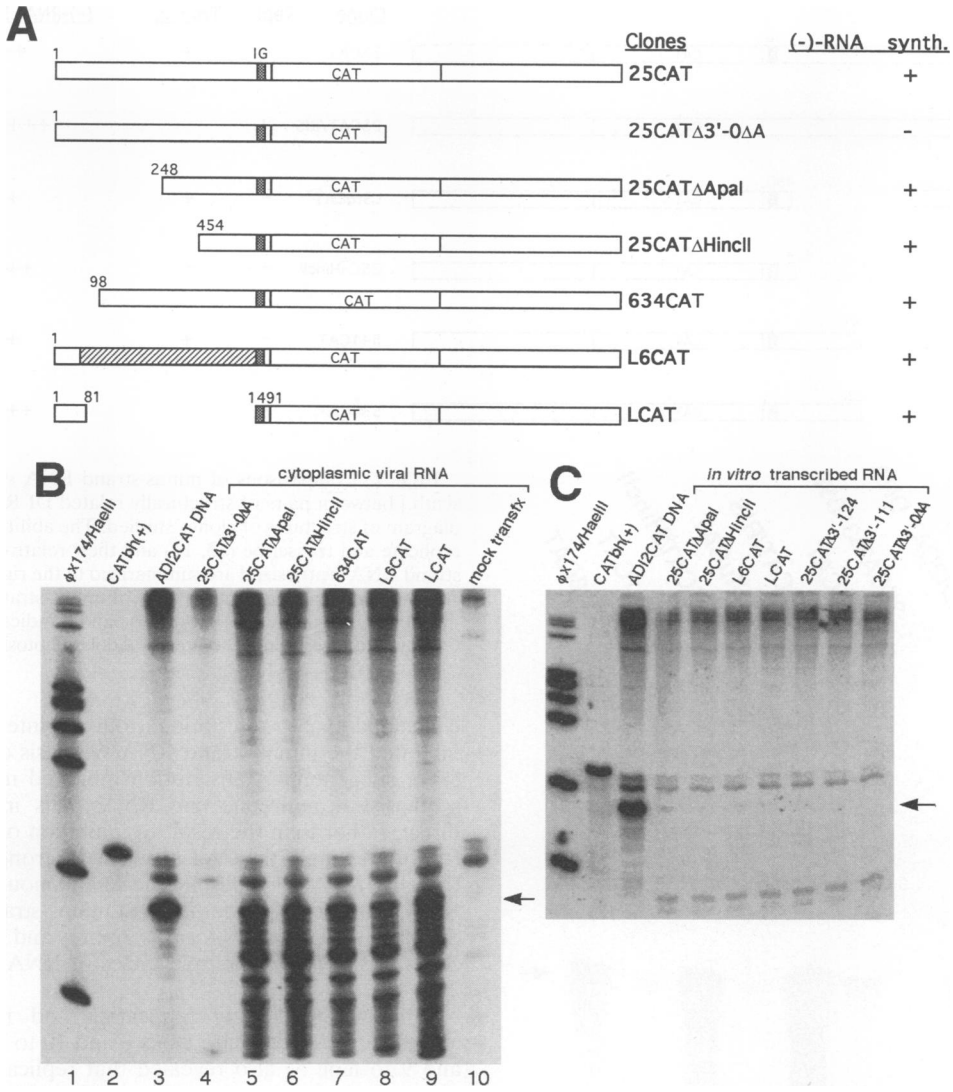

FIG. 6. Minus-strand RNA [(−)-RNA] synthesis of the 5′-end deletion clones. (A) Schematic diagram of structures of 5′-end deletion clones (13). The IG sequence on 25CAT is indicated. L6CAT contains the 5′-end sequence of mRNA 6 instead of DIssE and is shown as a hatched box. The abilities of these clones to synthesize minus-strand RNA are summarized to the right of each clone. (B) Analysis by RNase protection assay of minus-strand RNA synthesis by 5′-end deletion clones. (C) RNase protection assay of the in vitro-transcribed RNAs. The protected band is indicated by solid arrows. Computer images were generated by Adobe Photoshop, version 2.5.1 LE.

whether both genomic and subgenomic RNAs of MHV can serve as templates for minus-strand RNA synthesis and whether minus-strand RNA synthesis is the primary regulatory step of MHV RNA replication and transcription. A series of 25CAT-derived, 5′-end deletion clones constructed previously (13) were used for the study. Interestingly, all of the 5′-end deletion clones examined, which contain the intact 3′-end sequences, retained the ability to synthesize minus-strand RNA (Fig. 6B). Most strikingly, the 25CATΔHincII clone (Fig. 6B, lane 6), in which the 5′-end MHV sequence was almost completely deleted, made no less minus-strand RNA than did the other clones. To rule out the possibility of DNA or minus-strand RNA contamination in the transfected RNA samples, the various in vitro-transcribed, plus-strand DI RNAs were subjected directly to the same RNA isolation and RNase protection procedures; no protected RNA band was detected (Fig. 6C). In a parallel experiment, when these DI RNAs were transfected into mock-infected cells, no minus-strand RNA was detected (Fig. 5C, lane 6, and data not shown). Together, these results indicated that the detected minus-strand RNA was the result of RNA synthesis carried out by the helper virus. On the basis of the studies of the 5′- and 3′-end sequence requirements, we conclude that the recognition signal for minus-strand RNA synthesis resides within the 55 nt at the 3′ end plus poly(A) tail of the genomic RNA and that no specific 5′-end sequences are required for minus-strand RNA synthesis.

Subgenomic transcription inhibited minus-strand RNA synthesis. Previous studies suggested that subgenomic transcription from an internal promoter of MHV DI RNA inhibited RNA replication in *cis* (6). The mechanism of this inhibition is not clear. Preliminary studies also showed that 25CAT RNA, which transcribes a subgenomic CAT RNA (13), made less minus-strand RNA than DI RNAs which do not transcribe subgenomic RNAs (data not shown). Therefore, the inhibition

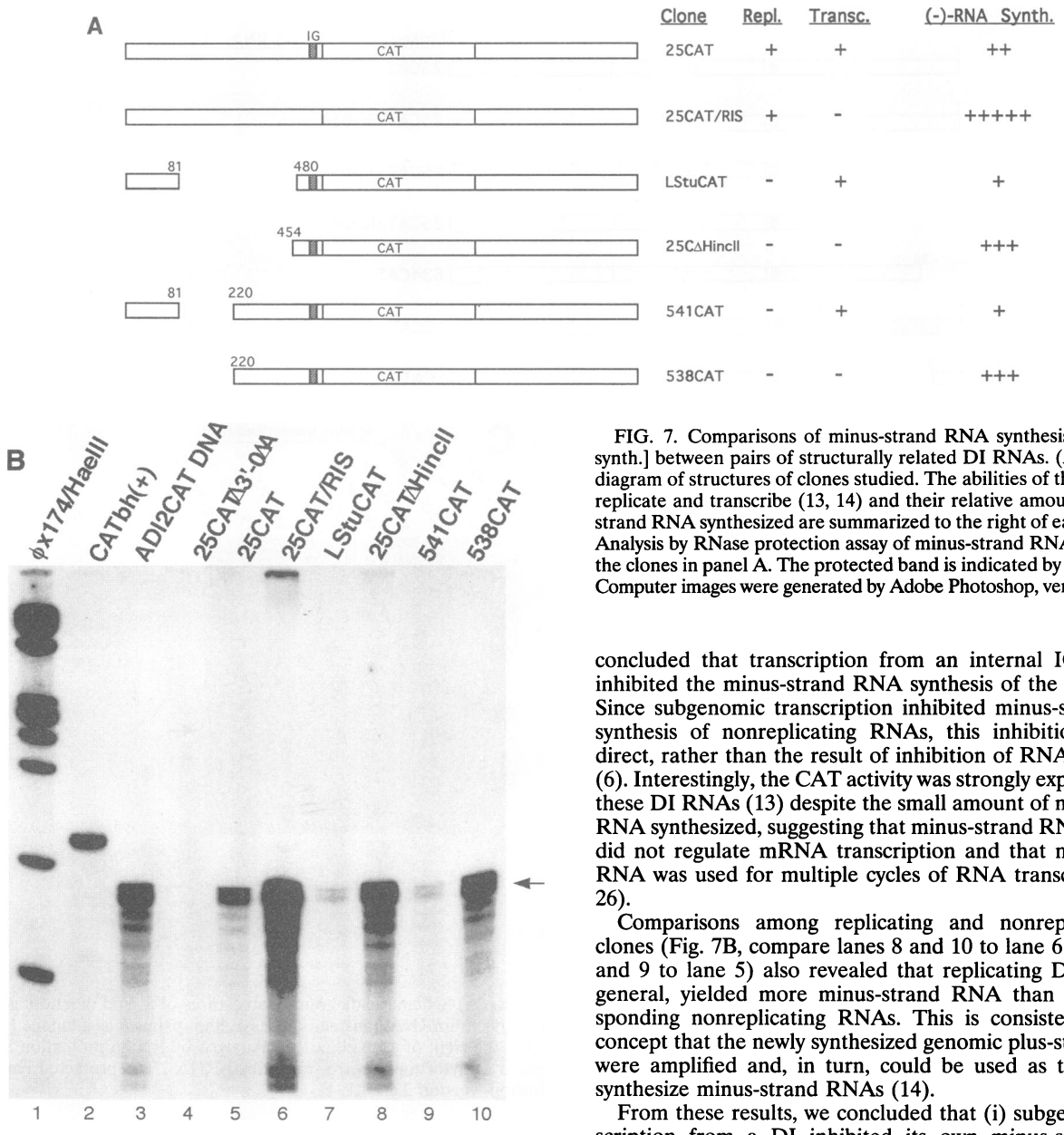

FIG. 7. Comparisons of minus-strand RNA synthesis [(−)−RNA synth.] between pairs of structurally related DI RNAs. (A) Schematic diagram of structures of clones studied. The abilities of these clones to replicate and transcribe (13, 14) and their relative amounts of minus-strand RNA synthesized are summarized to the right of each clone. (B) Analysis by RNase protection assay of minus-strand RNA synthesis by the clones in panel A. The protected band is indicated by a solid arrow. Computer images were generated by Adobe Photoshop, version 2.5.1 LE.

of DI RNA replication by subgenomic transcription from an internal promoter may be a result of inhibition of minus-strand RNA synthesis. To test this possibility, we studied several pairs of DI RNAs (Fig. 7A), which were structurally related but had different transcription or replication abilities, to compare the amounts of minus-strand RNA synthesized. For instance, 25CAT and 25CAT/RIS are almost identical in structure, except that the latter does not have the IG sequence and thus cannot transcribe a subgenomic CAT mRNA (13). Interestingly, 25CAT/RIS synthesized much more minus-strand RNA than 25CAT (Fig. 7B, lanes 5 and 6). In other pairs, the DI RNA clones (25CATΔHincII and 538CAT) which lacked the leader sequence and did not express CAT activity (13) made more minus-strand RNA than the corresponding clones (LStuCAT and 541CAT, respectively) which contained the leader and transcribed a subgenomic CAT mRNA (13) (Fig. 7B, lanes 7 and 8 and 9 and 10). Since these pairs of RNAs differed only in their abilities to transcribe the subgenomic CAT RNAs, we concluded that transcription from an internal IG sequence inhibited the minus-strand RNA synthesis of the same RNA. Since subgenomic transcription inhibited minus-strand RNA synthesis of nonreplicating RNAs, this inhibition must be direct, rather than the result of inhibition of RNA replication (6). Interestingly, the CAT activity was strongly expressed from these DI RNAs (13) despite the small amount of minus-strand RNA synthesized, suggesting that minus-strand RNA synthesis did not regulate mRNA transcription and that minus-strand RNA was used for multiple cycles of RNA transcription (24, 26).

Comparisons among replicating and nonreplicating DI clones (Fig. 7B, compare lanes 8 and 10 to lane 6 and lanes 7 and 9 to lane 5) also revealed that replicating DI RNAs, in general, yielded more minus-strand RNA than their corresponding nonreplicating RNAs. This is consistent with the concept that the newly synthesized genomic plus-strand RNAs were amplified and, in turn, could be used as templates to synthesize minus-strand RNAs (14).

From these results, we concluded that (i) subgenomic transcription from a DI inhibited its own minus-strand RNA synthesis, leading to reduced RNA replication, and (ii) RNA replication led to an increase in the amount of minus-strand RNA.

DISCUSSION

In this report, we have determined the sequence requirement for MHV minus-strand RNA synthesis and also revealed interesting insights into the mechanism of regulation of minus-strand RNA synthesis. This study was made possible by the development of a sensitive RNase protection assay to detect the presence of minus-strand RNA in MHV-infected, DI RNA-transfected cells. This system was sensitive enough to allow detection of minus-strand RNA synthesis from nonreplicating DI RNAs. This is important because the assay enabled us to examine the ability of an array of deletion clones which could not replicate to synthesize minus-strand RNA, thus establishing unequivocally the sequence requirement for mi-

nus-strand RNA synthesis. To our knowledge, this is the first successful determination of the sequence requirement for minus-strand RNA synthesis in vivo for any plus-strand RNA viruses. Previously, the promoter for minus-strand RNA synthesis of brome mosaic virus has been studied by in vitro RNA replication, which revealed that some RNA secondary structures at the 3′ end of RNA 3 are required for efficient brome mosaic virus minus-strand RNA synthesis in vitro (1). However, the promoter sequences have not been clearly defined, and it is not known whether these sequences are indeed the *cis*-acting signals for minus-strand RNA synthesis in vivo. For poliovirus and alphavirus, similar RNase protection assays have been used to detect viral minus-strand RNAs (12, 19) in a variety of studies of the regulation of RNA synthesis. However, the *cis*-acting signal for minus-strand RNA synthesis has not been determined. The RNase protection method optimized here will be useful for further studies of MHV transcription and replication.

The minimum signal for MHV minus-strand RNA synthesis was determined in this work to be within the 55 nt plus poly(A) tail at the 3′ end of MHV genome; no specific 5′-end sequences were required. This sequence requirement is significantly less stringent than that for MHV RNA replication, which includes 470 to 859 nt from the 5′ end and 436 nt from the 3′ end (and a 135-nt internal sequence for DI RNAs of the JHM strain) of MHV genome (7, 14, 27). Since RNA replication includes both plus- and minus-strand RNA synthesis, this result suggests that the most stringent regulation of MHV RNA synthesis occurs at the step of plus-strand RNA synthesis. It is interesting to note that the 3′-end sequence required for RNA replication is longer than that for minus-strand RNA synthesis, suggesting that plus-strand RNA synthesis may involve interactions between the 5′- and 3′-end sequences. Another significant insight gained from this study is that the leader RNA sequence, which has been shown to be required for subgenomic mRNA transcription (13) and RNA replication (7, 14, 27), is not required for minus-strand RNA synthesis. Thus, mRNA synthesis is most likely regulated at the level of plus-strand RNA synthesis but not minus-strand RNA synthesis. Therefore, this study is most consistent with the leader-primed transcription model, in which the leader RNA regulates transcription of plus-strand RNAs, in contrast to the model of discontinuous transcription, in which regulation of transcription occurs during minus-strand RNA synthesis. The results from this study also predict that minus-strand RNAs can be synthesized from both MHV genomic and subgenomic plus-strand RNAs, because all of these RNA species contain the 3′-end signal for minus-strand RNA synthesis. However, these minus-strand RNAs are not necessarily replicated into plus-strand RNA, since plus-strand RNA synthesis requires the leader sequences both in *cis* and in *trans* and additional sequences from the 5′ end of RNA genome (7, 13, 14, 29), which are not present in the subgenomic mRNAs. This conclusion was derived from the finding that minus-strand RNA was synthesized from some of the deletion clones which can neither replicate nor transcribe (Fig. 5 and 6). Thus, only the genomic-sized minus-strand RNA contained all of the necessary sequences for transcription and replication and is likely the only template used to synthesize functional plus-strand RNAs. Therefore, the subgenomic minus-strand RNAs may represent end products of RNA synthesis initiated from the 3′-end recognition signal for minus-strand RNA synthesis. The simplicity of the regulation of minus-strand RNA synthesis is consistent with the biological role of minus-strand RNA, since it is the first RNA species made and is made directly from incoming genomic RNA, when no viral proteins, other than RNA polymerase, are available. It is interesting to note that no cellular proteins have been found to bind to the 3′ end of the genomic RNA, while several factors bind to the 3′ end of minus-strand RNA and the 5′ end of plus-strand RNA (2), which are likely involved in plus-strand RNA synthesis.

In agreement with the previous reports (21, 23, 24, 26), the minus-strand RNA detected was found to exist in the ds RNA form. It is not clear whether some ss minus-strand RNAs are present in the infected cells or whether the ds RNA serves directly as the template for plus-strand RNA synthesis. Since the ds form of RNA is more stable than the ss form, the ds RNA form may provide stability to the minus-strand RNA in the infected cells. This is particularly important, in view of our finding that the 25CAT minus-strand RNA level remained constant from 2 h until at least 7 h p.i., suggesting that the minus-strand RNA synthesized was recycled continuously as a template to generate plus-strand RNAs throughout the replication cycle (see below). Thus, minus-strand RNA has to be very stable (23, 24); a ss form of minus-strand RNA would be vulnerable to intracellular RNase digestion and rendered relatively unstable. It is tempting to speculate that the ds RNA may be the template used for RNA synthesis.

Previously, MHV A59 and TGEV minus-strand RNAs have been detected starting at 2 to 3 h p.i. by either the metabolic labeling method or Northern blot analysis (23, 26). In this study, using the more sensitive RNase protection assay, we detected 25CAT minus-strand RNA as early as 20 min posttransfection or 1 h and 20 min p.i. (Fig. 4). This kinetics of minus-strand RNA synthesis indicates that viral RNA polymerase is synthesized immediately after virus entry. Unexpectedly, 25CAT minus-strand RNA synthesis peaked at 2 h p.i. and did not increase thereafter. In contrast, in the reported studies, MHV A59 and TGEV minus-strand RNA synthesis continued until 4 to 5 h p.i. (23, 26). To determine whether there is indeed a difference in the kinetics of minus-strand RNA synthesis between DI RNA and helper viral RNA will require further studies. Nevertheless, the limited amount of 25CAT minus-strand RNA synthesized still led to a high level of CAT gene expression (13), indicating that the minus-strand RNA was used as a template for many cycles to synthesize subgenomic mRNAs, consistent with the previous results (24, 26). The minus-strand RNA template may also be reused for many rounds of genome replication (24, 26).

Our studies here also revealed unexpected effects of transcription and replication on minus-strand RNA synthesis. All of the DI RNAs which transcribe a subgenomic mRNA synthesized a smaller amount of minus-strand RNA than those which do not transcribe, suggesting that the minus-strand RNA synthesis was inhibited by transcription from the same DI RNA. Similarly, it has been shown that subgenomic transcription from a DI RNA inhibited its own RNA replication (6). This inhibitory effect was observed only in *cis* (i.e., transcription did not inhibit the replication of a separate DI RNA) (6). Since the inhibition of minus-strand RNA synthesis was observed in nonreplicating DI RNA clones (LStuCAT and 541CAT), it is most likely that the inhibition by subgenomic transcription on minus-strand RNA synthesis was direct, and the inhibited minus-strand RNA synthesis then led to reduced RNA replication. The mechanism of inhibition on minus-strand RNA synthesis by subgenomic transcription is not clear. Nevertheless, this finding suggests that subgenomic mRNAs, which also contain the recognition signal for minus-strand RNA synthesis, are poor templates for minus-strand RNA synthesis, again indicating that the amounts of mRNAs are not regulated by the amounts of minus-strand RNA, in contrast to a previous suggestion (26). One possible explanation for the

poor ability of subgenomic mRNA to synthesize minus-strand RNA is that once mRNAs are made, they are separated from the RNA replication or transcription machinery and used for translation instead of minus-strand RNA synthesis. In contrast, the DI RNAs which could replicate yielded more minus-strand RNAs than those which could not, suggesting that the replicated RNA is used as a template to synthesize minus-strand RNA. These studies together suggest that the genomic RNA can serve as a template for minus-strand RNA synthesis, while subgenomic mRNAs are inefficient templates. Thus, it is most likely that minus-strand RNA was synthesized predominantly through the genomic, rather than the subgenomic, plus-strand RNA template. This study also raised an interesting question, i.e., why viral subgenomic mRNA synthesis does not inhibit wild-type genomic RNA replication. The data in our studies will argue that subgenomic and genomic RNA syntheses are temporally regulated, so that they are synthesized at different time points after infection. Further characterization of minus-strand RNA will likely provide additional insights into the mechanism of MHV RNA transcription and replication.

ACKNOWLEDGMENTS

We thank Xuming Zhang and King-Song Jeng for helpful discussions and valuable advice. We also thank Daphne Shimoda for editorial assistance.

This work was supported by grant AI-19244 from the National Institutes of Health. M.M.C.L. is an investigator of the Howard Hughes Medical Institute.

REFERENCES

1. **Dreher, T. W. and T. C. Hall.** 1988. Mutational analysis of the sequence and structural requirements in brome mosaic virus RNA for minus strand promoter activity. J. Mol. Biol. **201**:31–40.
2. **Furuya, T., and M. M. C. Lai.** 1993. Three different cellular proteins bind to complementary sites on the 5′-end-positive and 3′-end-negative strands of mouse hepatitis virus RNA. J. Virol. **67**:7215–7222.
3. **Hirano, N., K. Fujiwara, S. Hino, and M. Matumoto.** 1974. Replication and plaque formation of mouse hepatitis virus (MHV-2) in mouse cell line DBT culture. Arch. Gesamte Virusforsch. **44**:298–302.
4. **Hofmann, M. A., and D. A. Brian.** 1991. The 5′ end of coronavirus minus-strand RNAs contains a short poly(U) tract. J. Virol. **65**: 6331–6333.
5. **Hofmann, M. A., P. B. Sethna, and D. A. Brian.** 1990. Bovine coronavirus mRNA replication continues throughout persistent infection in cell culture. J. Virol. **64**:4108–4114.
6. **Jeong, Y. S., and S. Makino.** 1992. Mechanism of coronavirus transcription: duration of primary transcription initiation activity and effects of subgenomic RNA transcription on RNA replication. J. Virol. **66**:3339–3346.
7. **Kim, Y. N., Y. S. Jeong, and S. Makino.** 1993. Analysis of *cis*-acting sequences essential for coronavirus defective interfering RNA replication. Virology **197**:53–63.
8. **Lai, M. M. C.** 1990. Coronavirus: organization, replication and expression of genome. Annu. Rev. Microbiol. **44**:303–333.
9. **Lai, M. M. C., and S. A. Stohlman.** 1978. RNA of mouse hepatitis virus. J. Virol. **26**:236–242.
10. **Lau, E. T., R. Y. C. Kong, and K. S. E. Cheah.** 1993. A critical assessment of the RNase protection assay as a means of determining exon sizes. Anal. Biochem. **209**:360–366.
11. **Lee, H.-J., C.-K. Shieh, A. E. Gorbalenya, E. V. Koonin, N. La Monica, J. Tuler, A. Bagdzhadzhyan, and M. M. C. Lai.** 1991. The complete sequence (22 kilobases) of murine coronavirus gene 1 encoding the putative proteases and RNA polymerase. Virology **180**:567–582.
12. **Lemm, J. A., and C. M. Rice.** 1993. Assembly of functional Sindbis virus RNA replication complexes: requirement for coexpression of P123 and P34. J. Virol. **67**:1905–1915.
13. **Liao, C.-L. and M. M. C. Lai.** 1994. The requirement of 5′-end genomic sequence as an upstream *cis*-acting element for coronavirus subgenomic mRNA transcription. J. Virol. **68**:4727–4737.
14. **Lin, Y.-J., and M. M. C. Lai.** 1993. Deletion mapping of a mouse hepatitis virus defective interfering RNA reveals the requirement of an internal and discontiguous sequence for replication. J. Virol. **67**:6110–6118.
15. **Makino, S., M. Joo, and J. K. Makino.** 1991. A system for study of coronavirus mRNA synthesis: a regulated, expressed subgenomic defective interfering RNA results from intergenic site insertion. J. Virol. **65**:6031–6041.
16. **Makino, S., C.-K. Shieh, L. H. Soe, S. C. Baker, and M. M. C. Lai.** 1988. Primary structure and translation of a defective interfering RNA of murine coronavirus. Virology **166**:550–560.
17. **Manaker, R. A., C. V. Piczak, A. A. Miller, and M. F. Stanton.** 1961. A hepatitis virus complicating studies with mouse leukemia. J. Natl. Cancer Inst. **27**:29–51.
18. **Masters, P. S., C. A. Koetzner, C. A. Kerr, and Y. Heo.** 1994. Optimization of targeted RNA recombination and mapping of a novel nucleocapsid gene mutation in the coronavirus mouse hepatitis virus. J. Virol. **68**:328–337.
19. **Novak, J. E., and K. Kirkegaard.** 1991. Improved method for detecting poliovirus negative strands used to demonstrate specificity of positive-strand encapsidation and the ratio of positive to negative strands in infected cells. J. Virol. **65**:3384–3387.
20. **Pachuk, C. J., P. J. Bredenbeek, P. W. Zoltick, W. J. M. Spaan, and S. R. Weiss.** 1989. Molecular cloning of the gene encoding the putative polymerase of mouse hepatitis virus, strain A59. Virology **171**:141–148.
21. **Perlman, S., D. Ries, E. Bolger, L. J. Chang, and C. M. Stoltzfus.** 1986. MHV nucleocapsid synthesis in the presence of cycloheximide and accumulation of negative strand MHV RNA. Virus Res. **6**:261–272.
22. **Sambrook, J., E. F. Fritsch, and T. Maniatis.** 1989. Molecular cloning: a laboratory manual, 2nd ed. Cold Spring Harbor Laboratory Press, Cold Spring Harbor, N.Y.
23. **Sawicki, S. G., and D. L. Sawicki.** 1986. Coronavirus minus-strand RNA synthesis and effect of cycloheximide on coronavirus RNA synthesis. J. Virol. **57**:328–334.
24. **Sawicki, S. G., and D. L. Sawicki.** 1990. Coronavirus transcription: subgenomic mouse hepatitis virus replicative intermediates function in RNA synthesis. J. Virol. **64**:1050–1056.
25. **Sethna, P. B., M. A. Hofmann, and D. A. Brian.** 1991. Minus-strand copies of replicating coronavirus mRNAs contain antileaders. J. Virol. **65**:320–325.
26. **Sethna, P. B., S.-L. Hung, and D. A. Brian.** 1989. Coronavirus subgenomic minus-strand RNAs and the potential for mRNA replicons. Proc. Natl. Acad. Sci. USA **86**:5626–5630.
27. **van der Most, R. G., P. J. Bredenbeek, and W. J. M. Spaan.** 1991. A domain at the 3′ end of the polymerase gene is essential for encapsidation of coronavirus defective interfering RNAs. J. Virol. **65**:3219–3226.
28. **van der Most, R. G., R. J. de Groot, and W. J. M. Spaan.** 1994. Subgenomic RNA synthesis directed by a synthetic defective interfering RNA of mouse hepatitis virus: a study of coronavirus transcription initiation. J. Virol. **68**:3656–3666.
29. **Zhang, X., C.-L. Liao, and M. M. C. Lai.** 1994. Coronavirus leader RNA regulates and initiates subgenomic RNA transcription both in *trans* and in *cis*. J. Virol. **68**:4738–4746.